

O. Golikov\* , Y. Darkhan , T. Yerlanov 

Al-Farabi Kazakh National University, Almaty, Kazakhstan;

\*e-mail: golikov@physics.kz

*(Received 26 January 2023; received in revised form 17 April 2023; accepted 03 May 2023)*

## A semi-automatic examination of CO<sub>2</sub> structures in thin films at low temperatures

**Abstract.** The aim of this paper is to study the IR spectra of thin films of a mixture of carbon dioxide and water obtained via vapor deposition in the temperature range of 11-180 K. Based on the analysis of the spectra, we examine the formation of hydrates and clathrates that are of interest to modern condensed matter physics. To carry out this research, the methods of IR spectroscopy, mass spectroscopy, and optical analysis of the thin films formed were utilized. Fourier transform infrared spectroscopy is one of the most reliable methods for the identification of the molecular composition and structural states of molecular mixtures. Additional tools, such as mass spectroscopy and interference patterns, were used to confirm the formation of specific structures in the carbon dioxide and water mixture. During the experiments, CO<sub>2</sub> hydrate and gas hydrate structures formed in the mixture. The gas hydrates that formed in the mixture can be classified as sI-type hydrates. The hydrate compounds hold CO<sub>2</sub> molecules in their structures, preventing them from sublimating at 93 K (the sublimation temperature of unbound CO<sub>2</sub> at a pressure of  $P = 0.5 \mu\text{Torr}$ ). At the same time, the sublimation temperature of CO<sub>2</sub> molecules bound in hydrate structures becomes equal to 147-150 K. For the selected concentration of CO<sub>2</sub> (25%) – H<sub>2</sub>O (75%), the changes in the observed spectra and the data obtained using mass spectroscopy indicate incomplete hydration of the mixture. Some of the CO<sub>2</sub> molecules remain unbound and sublimate earlier. The increase in the refractive index as the concentration of H<sub>2</sub>O in the mixture approaches 25% indicates the growth of structures that are denser compared to amorphous CO<sub>2</sub> condensates and amorphous H<sub>2</sub>O ice. The results expand the current knowledge of the clathrate and hydrate formation processes in mixtures of CO<sub>2</sub> and H<sub>2</sub>O, their physical characteristics, and the emergence of certain characteristics depending on the method of formation.

**Key words:** Cryocondensation, hydrate, PVD, carbon dioxide, thin films.

### Introduction

Capturing and storing carbon dioxide molecules is one of the most promising strategies to combat global warming, a potential environmental disaster [1–3]. It is known that CO<sub>2</sub> molecules present at a depth of more than 400 meters underwater change their shape and form gas hydrates, which block their evaporation to the water surface and the atmosphere, thus avoiding the formation of greenhouse gases. This concept has become one of the key factors in reducing CO<sub>2</sub> emissions [4]. In addition, gas hydrates contain a large amount of relatively clean energy compared with other conventional sources of hydrocarbons [5]. Besides, natural gas can be obtained from gas hydrates, as described in several articles on a number of advanced mining technologies [6, 7]. However, it is important to know the conditions under which CO<sub>2</sub> molecules are able to create gas hydrate structures and remain in them.

Gas hydrates are compounds formed by water molecules connected by hydrogen bonding in a spherical shape, which is stabilized by a guest molecule (NO<sub>2</sub>, Ar, CO<sub>2</sub>). The guest molecule is “locked” inside the H<sub>2</sub>O lattice during the stabilization process and stays inside it for a long time until the integrity of the hydrogen bond is broken [8]. A unique physical feature of gas hydrates is guest selectivity [9, 10], which is of particular importance for the development of the technology of separation and storage of certain gases. In other words, it can be said that CO<sub>2</sub> molecules, or any guest molecules, can be easily captured even in mixed gases. Furthermore, gas hydrates exhibit extremely high gas storage performance in the created structure [11–13].

The concept of storing CO<sub>2</sub> molecules in so-called hydrate sealing was proposed in the work of Koide [14]. Later, this effect was described in more detail in Tohidi’s paper [15]. The application of this effect was described in [16][17][18] in which the

authors considered the possibility and technical feasibility of storing carbon dioxide molecules using gas hydrate-based capture.

A number of works concerning gas hydrates also focus on more fundamental research, for example, studying the speed of hydrate structure formation [19, 20], clathrate (gas hydrate) separation based on capture technology in a carbon Integrated Gasification Combined-Cycle [21–24], and the effect of temperature and pressure on the formation of gas hydrates [25]. Studying the behavior and properties of the formation of hydrate and gas hydrate structures is still one of the relevant research topics in the field of ecology and energy [26–29].

This paper includes a study of the formation process and the main spectral characteristics of thin films and gas hydrate structures of CO<sub>2</sub> molecules obtained using the vapor deposition method. Fourier transform infrared spectroscopy (FTIR spectroscopy) in the mid-IR range (400–4200 1/cm) and mass spectroscopy were chosen as the main tools to analyze the obtained samples. FTIR was chosen due to several considerations: firstly, this method is used by researchers and has demonstrated its effectiveness in many scientific fields, including the study of thin films and cryocondensates [30–32]; secondly, in the mid-IR range, it is possible to observe most of the spectral peaks that are of interest to us and are mentioned in the works of other authors, we are interested in [33–35]. The mass spectroscopy method was only used in our research for verification.

## Materials and Methods

The thin films of the samples of CO<sub>2</sub> + H<sub>2</sub>O compounds were formed using the physical vapor deposition (PVD) method [36]. The deposition was performed at T=11 K on a special, gold-coated substrate of a semi-automatic cryovacuum spectrophotometer unit, shown in figure 1. The vapor deposition method is one of the most effective methods of obtaining thin films of cryocondensates in well-controlled structural phase states [37–39]. It is also widely used to study the physical properties of compounds at low and ultra-low temperatures [39–43].

The presence of the Extorr XT100 gas analyzer (Extorr Inc., USA), a quadrupole residual gas analyzer, and a heating element built into the substrate permits quantitative determination of the components during their sublimation. In this research, the spectra were obtained in the temperature range of 11–200 K at a pressure of P=0.5 μTorr. The

thickness of the films remained the same throughout all the experiments at all condensation temperatures.

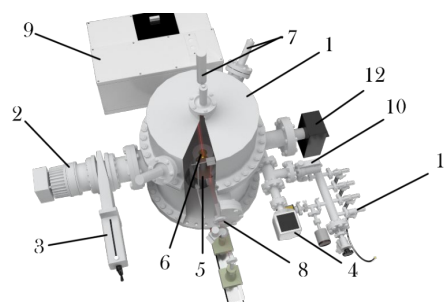


**Figure 1** – Cryovacuum condensation experimental setup: 1) vacuum chamber, 2) vacuum pump Turbo-V-301, 3) vacuum gate valve CFF-100, 4) pressure detector FRG-700, 5) Gifford-McMahon refrigerator, 6) substrate, 7) photo multiplier, laser interferometer, 8) light source, optical channel, 9) IR-spectrometer, 10) high-precision gas supply leak into the chamber; 11) gas leak into the mixture production system; 12) The Extorr XT100

An automated temperature control module made with the LabView software package (National Instruments, USA) is another important feature of the unit. This module connects the cooling substrate of the Gifford-McMahon machine, the heater, the temperature sensor DT-670, and the PID controller of the LakeShore 325 thermal controller (LakeShore, USA). It helps to reach the required temperatures more quickly and further stabilize them near the reference point at which the spectral characteristics are obtained. In addition, as soon as the reference point is reached, the module switches off the Gifford-McMahon machine, which creates vibration oscillations when it is working.

The spectral characteristics of the samples were detected using the FSM 2203 FTIR spectrometer (INFRASPEK, Russia), which has a maximum spectral resolution of 0.125 1/cm and a spectral range of 370–7800 1/cm.

The refractive index and thickness of the thin film deposited on the substrate are determined using the interference patterns obtained from two beams of a semiconductor laser formed by fission and detected using a P25A photomultiplier tube (Sens-Tech, UK). The angles of incidence of the two beams are  $\alpha_1 \approx 0^\circ$  and  $\alpha_2 \approx 45^\circ$ . The laser wavelength is  $\lambda=406$  nm, and the maximum sensitivity of the PMT is also in the range of about 400 nm, which is important for obtaining high-quality interference patterns. The calculation of the refractive indexes is performed according to the formula:

$$n = \sqrt{\frac{\sin^2 \alpha_2 - \left(\frac{t_1}{t_2}\right)^2 \sin^2 \alpha_1}{1 - \left(\frac{t_1}{t_2}\right)^2}}$$

where  $t_1$  and  $t_2$  are the periods, and  $\alpha_1$  and  $\alpha_2$  are the angles of incidence of the first and second lasers, respectively.

The formation and path of the laser beam during the experiment are demonstrated in the form of a 3D model shown in figure 2. The data recorded from the lasers were used to check the direction of evaporation: does the sublimation process really start from the substrate, on which the sample is located, or is it the exhaust of residual gases from another part of the vacuum chamber? Since vapor has a strong influence on the path of the beam, the lasers began to spike when the sublimation process began from the substrate.

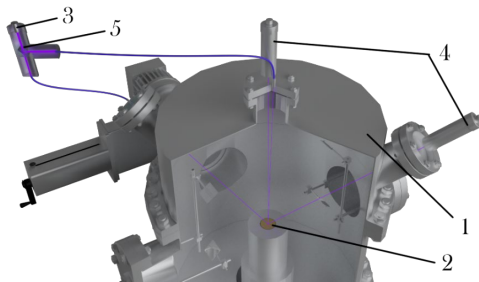


**Figure 2** – 3D-model of the laser beam formation during the cryovacuum condensation: 1) vacuum chamber; 2) substrate; 3) laser; 4) photomultipliers; 5) optical splitter

During the research, mixtures in different concentration ratios of H<sub>2</sub>O and CO<sub>2</sub> were created. For this purpose, a flow system was used (figure 1, 11). When determining the necessary proportions of

water and carbon dioxide, we relied on Dalton's law of partial pressure. In general, the sequence of the sample creation looks like this:

1. The small volume of the leakage system, in which the mixture is subsequently created, is drained.
2. The first substance (H<sub>2</sub>O in our case) of the future mixture, which has a lower saturated vapor pressure, is injected into the drained volume.
3. The second substance is injected. After the first and second substances are injected, their ratios are determined according to the pressure values.
4. The mixture created is injected into the vacuum chamber and deposited on the substrate.

CO<sub>2</sub> of 99.999% purity (ISHAN TEHNO-GAS LLP, Almaty, Kazakhstan) was used in experiments. It had a maximum oxygen fraction not exceeding 0.0005%, water vapors not exceeding 0.0007%, and distilled water with a mass fraction of residue after evaporation not exceeding 0.005% of the volume was used in experiments.

## Results and Discussion

### Refractive index and growth rate

During the experiment, the condensate growth rate and refractive indices for a number of different concentrations of CO<sub>2</sub> and H<sub>2</sub>O were determined at the temperatures of T=11 K, T=45 K, T=80 K, and T=110 K. The data obtained using the interference patterns of two laser beams for the mixtures of water and carbon dioxide are presented in table 1 and table 2. An increase in the refractive index can be observed as the concentration of water in the mixture approaches 25% (H<sub>2</sub>O(25%) + CO<sub>2</sub>(75%), table 2). This pattern may indicate the growth of structures that are denser than amorphous carbon dioxide condensates or amorphous water ice. This interesting pattern can be observed in other gas hydrate mixtures as well [42].

**Table 1** – Film deposition and refractive rates versus temperature.

| Prepared mixture for condensation             | Temperature, K | Deposition rate, μm/s | Refractive index, n |
|---|----------------|-----------------------|---------------------|
| H <sub>2</sub> O(85%) + CO <sub>2</sub> (15%) | 11             | 0.0167                | 1.2567              |
| H <sub>2</sub> O(85%) + CO <sub>2</sub> (15%) | 45             | 0.0141                | 1.3293              |
| H <sub>2</sub> O(85%) + CO <sub>2</sub> (15%) | 80             | 0.0110                | 1.4044              |
| H <sub>2</sub> O(85%) + CO <sub>2</sub> (15%) | 110            | 0.0052                | 1.2875              |
| CO <sub>2</sub> (100%)                        | 11             | 0.0230                | 1.2320              |
| CO <sub>2</sub> (100%)                        | 45             | 0.0138                | 1.3935              |
| H <sub>2</sub> O(100%)                        | 11             | 0.0167                | 1.2231              |

**Table 2** – The film index of refraction on the concentration of the mixture.

| Substance                                     | Temperature, K | Deposition rate, $\mu\text{m/s}$ | Refractive index, n |
|---|----------------|----------------------------------|---------------------|
| CO <sub>2</sub>                               | 11             | 0.0118                           | 1.2320              |
| H <sub>2</sub> O(25%) + CO <sub>2</sub> (75%) | 11             | 0.0114                           | 1.3381              |
| H <sub>2</sub> O(50%) + CO <sub>2</sub> (50%) | 11             | 0.0176                           | 1.2860              |
| H <sub>2</sub> O(75%) + CO <sub>2</sub> (25%) | 11             | 0.0181                           | 1.2760              |
| H <sub>2</sub> O(80%) + CO <sub>2</sub> (20%) | 11             | 0.0166                           | 1.2703              |
| H <sub>2</sub> O(85%) + CO <sub>2</sub> (15%) | 11             | 0.0166                           | 1.2708              |
| H <sub>2</sub> O(90%) + CO <sub>2</sub> (10%) | 11             | 0.0155                           | 1.2539              |
| H <sub>2</sub> O(95%) + CO <sub>2</sub> (5%)  | 11             | 0.0173                           | 1.2330              |
| H <sub>2</sub> O(100%)                        | 11             | 0.0167                           | 1.2231              |

Moreover, the data in table 1 suggest that the refractive index for the mixture of H<sub>2</sub>O(85%) + CO<sub>2</sub>(15%) increases up to 80 K and then decreases at 110 K as the condensation temperature rises. This is most likely related to the fact that the sublimation temperature of free CO<sub>2</sub> molecules at a pressure of  $P=0.5\mu\text{Torr}$  is 93 K.

### FTIR spectroscopy

The values of the frequencies of asymmetric vibrations ( $\nu_3$  mode) are most often used to identify and describe gas, solid, hydrate, and gas hydrate

formations of carbon dioxide in various compounds [33-35]. Our study is focused on it. Figure 3 shows the vibrational modes of two ranges. The first range, 2265-2295 1/cm (figure 3(a)), is typical of the asymmetric vibrations of the O<sup>16</sup>C<sup>13</sup>O<sup>16</sup> isotope. The second range, 2310-2390 1/cm (figure 3 (b)), is typical of pure O<sup>16</sup>C<sup>12</sup>O<sup>16</sup> carbon dioxide molecules. Oscillations at higher frequencies (2279 1/cm and 2283 1/cm) can most likely be classified as vibrations of small carbon dioxide structures ( $5^{12}$ ) for O<sup>16</sup>C<sup>13</sup>O<sup>16</sup> molecules, while vibrations at 2275 1/cm can be classified as vibrations of large structures ( $5^{12}6^2$ ).

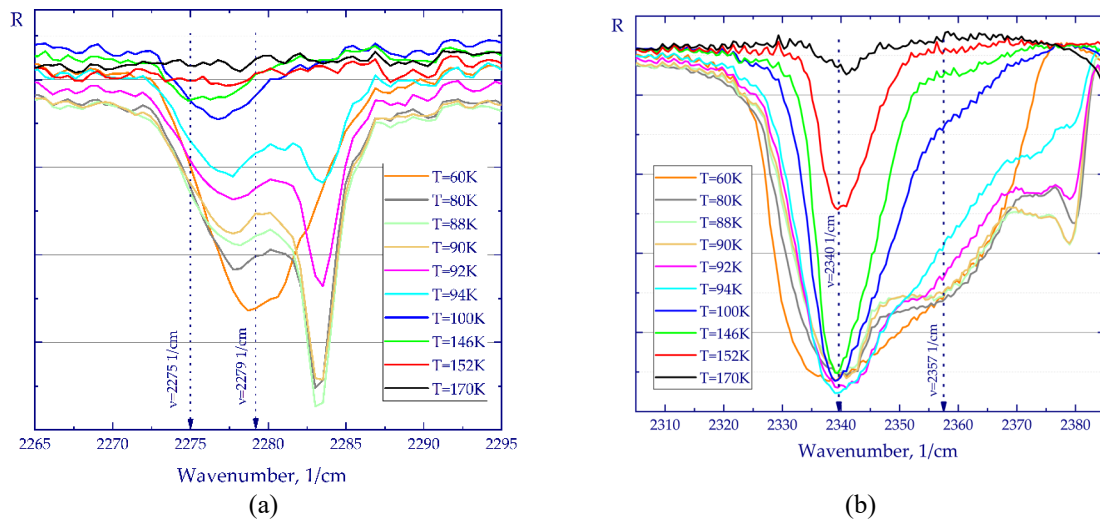


**Figure 3** – Carbon dioxide spectrum dependent on the temperature:  
 (a) in the vibrational region 2265-2295 1/cm  $\nu_3$  of O<sup>16</sup>C<sup>13</sup>O<sup>16</sup>;  
 (b) in the vibrational region 2310-2380 1/cm  $\nu_3$  of O<sup>16</sup>C<sup>12</sup>O<sup>16</sup> molecules

Asymmetric vibrational spectra at frequencies of 2275 1/cm and 2280 1/cm reflect a correlation with the FTIR spectra of sI-type O<sup>16</sup>C<sup>13</sup>O<sup>16</sup> gas hydrates as reported by the researchers in [44]. Besides, in

addition to the peaks, the presence of a shift towards a decrease in the wave number with an increase in the substrate temperature indicates a correlation as well. The bifurcation of the main peak at an additional



frequency of 2283 1/cm is an intriguing feature. This frequency can also be attributed to the vibrations of the  $O^{16}C^{13}O^{16}$  isotope molecules [45]. It can be seen that the intensity of this oscillation weakens as the temperature increases, and after 94 K, it disappears. This can be related to the fact that this peak belongs to the vibrations of free molecules of  $O^{16}C^{13}O^{16}$  that have not formed a hydrogen bond with  $H_2O$  molecules; therefore, they evaporate as soon as the sublimation temperature of pure carbon dioxide is reached. The fact that this peak belongs to the frequencies of vibration of gaseous and ice  $O^{16}C^{13}O^{16}$  is stated in [33] as well.

The asymmetric  $\nu_3$  stretching-mode spectra for the  $O^{16}C^{12}O^{16}$  molecules that we observed in the experiments are shown in figure 3(b) (frequencies of 2340 1/cm and 2357 1/cm). In [33], the vibrational peak at the frequency of 2360 1/cm is classified as an oscillation of pure gaseous  $O^{16}C^{12}O^{16}$ . The vibrational peak at the frequency of 2340 1/cm is interpreted differently in different sources because gas, ice, and hydrate  $O^{16}C^{12}O^{16}$  show asymmetric vibrations at this frequency [33, 46, 47]. We assume that this peak belongs to the  $O^{16}C^{12}O^{16}$  sI-type gas hydrate as we observe the presence of carbon dioxide molecules after the sublimation temperature typical of  $CO_2$  ices and gases. The peak at 2380 1/cm is an uncharacteristic peak of the  $O^{16}C^{13}O^{16}$  isotope [45] and belongs to the gas structure of carbon dioxide molecules that are not bound to  $H_2O$ .

During the experiments, the  $(2\nu_1 + \nu_3)$  FR1 oscillations were not observed. However, their expected position is shown in [33]. The absence of these peaks during our experiments is most likely related to the fact that water ice demonstrates a high absorption intensity in this range, thus preventing the weaker  $(2\nu_1 + \nu_3)$  FR1 peaks from being detected at frequencies of 3580-3620 1/cm.

Figure 4 depicts the  $(\nu_1 + \nu_3)$  FR1 absorption peaks. Similar to the vibrational peak at a frequency of 2340 1/cm, this region is very difficult to interpret due to the vibrational spectra of gas, hydrate, and clathrate  $CO_2$  and  $H_2O$  compounds being very similar. Based on what is stated in [33, 35, 44], we assume that the peaks at 3709 1/cm and the absorption at 3704 1/cm can be classified as characteristic peaks and absorption of a  $CO_2$  hydrate.

An interesting dependence can be seen in the three-dimensional representation of the  $\nu_3$  vibrational spectra shown in figure 5. We stress again that the process of sublimation of free carbon dioxide molecules under the pressure of  $P = 0.5\mu\text{Torr}$  begins

at the temperature of  $T = 94$  K [48]. Nevertheless, it can be observed that  $\nu_3$  asymmetric vibrations for  $CO_2$  molecules at 2340 1/cm occur up to 150 K. This observation may indicate that some of the carbon dioxide molecules remain in the mixture after reaching the sublimation temperature, apparently trapped in the gas hydrate structures.

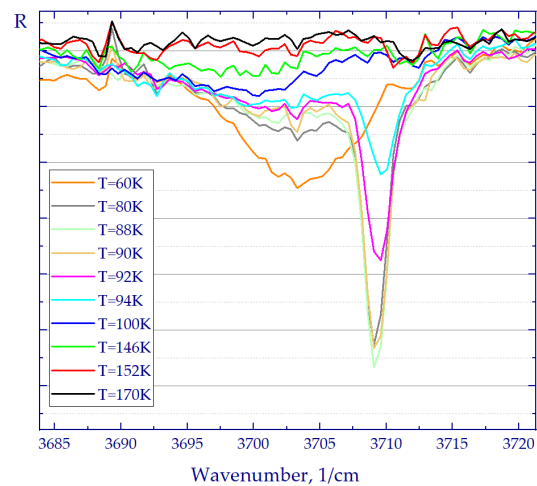


**Figure 4** – Carbon dioxide spectrum dependent on the temperature in the  $(\nu_1 + \nu_3)$  FR1 vibrational region

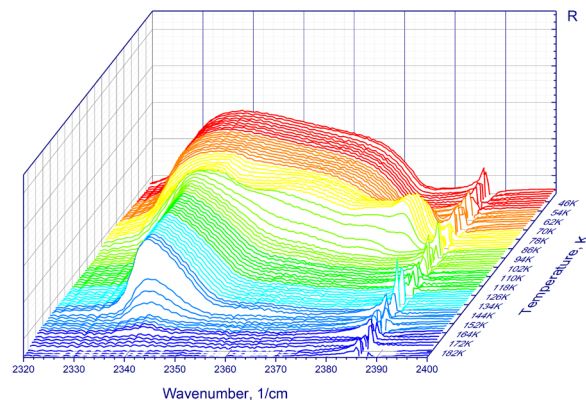


**Figure 5** – Temperature evolution of the  $\nu_3$  vibrational mode of  $CO_2$  for the band at the frequencies of 2320 1/cm – 2400 1/cm

It is also possible to observe that the shape of the vibrational peak in the frequency range of 2320-2380 1/cm changes after reaching a temperature of 94 K. This is most likely connected with the evaporation of the molecules of the  $O^{16}C^{13}O^{16}$  free isotope, which is either free or trapped in small structures ( $5^{12}$ ). However, further research is required in order to be certain that these peaks belong to the  $O^{16}C^{13}O^{16}$  isotope.

### Mass spectroscopy

The mass spectra of the H<sub>2</sub>O + CO<sub>2</sub> mixture obtained during the sublimation processes are shown in figure 6. They were obtained mainly to identify the sublimation agent by its molar mass. It can be seen that, to a certain extent, the sublimation of carbon dioxide and water molecules proceeds at their typical temperatures at a pressure of  $P = 0.5\mu\text{Torr}$ : for CO<sub>2</sub>, the temperature is about 93 K (insignificant sublimation is observed), and for H<sub>2</sub>O, the temperature is about 172 K (complete sublimation of water molecules).

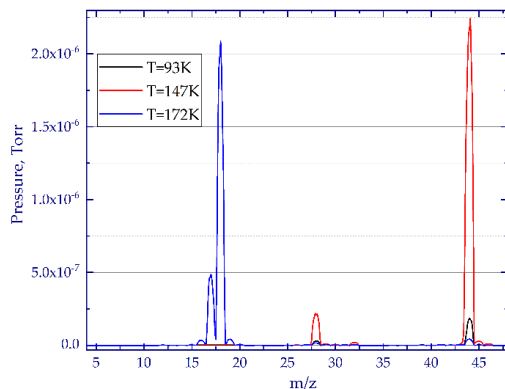


**Figure 6** – Mass spectra of the condensation mixture of water and CO<sub>2</sub>

However, the same figure shows that some of the carbon dioxide molecules remain in the mixture even after reaching its sublimation temperature. The only way to explain this phenomenon is the formation of hydrate structures that prevent the sublimation of some of the CO<sub>2</sub> molecules, keeping them in the mixture. It is assumed that these structures are most likely gas hydrates and that the CO<sub>2</sub> molecules are “stuck” in the spherically bound water molecules that trap them and prevent them from sublimating at 93 K. Moreover, the FTIR spectra presented above suggest that CO<sub>2</sub> remains in the mixture after overcoming the sublimation temperature.

### Conclusion

The experiments carried out in this research were aimed at studying and further identifying the

structural formations obtained via PVD in a mixture of H<sub>2</sub>O + CO<sub>2</sub>. Several methods were used to achieve the goals: mass spectroscopy, optical studies, and FTIR spectroscopy. The results allow us to conclude the following:

- During the experiments, the formation of CO<sub>2</sub> hydrate and gas hydrate structures occurred in the mixture.

- The gas hydrates formed can be classified as sI-type hydrates.

- The hydrate compounds formed hold CO<sub>2</sub> molecules in their structures, preventing them from sublimating at 93 K (the sublimation temperature of free CO<sub>2</sub> at a pressure of  $P = 0.5\mu\text{Torr}$ ). In this case, the sublimation temperature of CO<sub>2</sub> molecules that form hydrate structures becomes equal to 147-150 K.

- For the chosen concentration of CO<sub>2</sub> (25%) – H<sub>2</sub>O (75%), the changes in the spectra obtained and the data collected using mass spectroscopy indicate incomplete hydration of the mixture. Some of the CO<sub>2</sub> molecules remain free and sublime earlier.

- The increase in the refractive index as the concentration of H<sub>2</sub>O in the mixture approaches 25% indicates the growth of structures that are denser compared to amorphous CO<sub>2</sub> condensates and amorphous H<sub>2</sub>O ice.

Of course, in order to study the conditions of the formation of hydrate and gas hydrate CO<sub>2</sub> compounds more accurately, further research is required. Studies in the field of hydrate and clathrate structures do not provide sufficient data on the physical characteristics of their composition and the emergence of certain characteristics depending on the method of formation of a hydrate or clathrate. This is why it is important to explore this field from different angles, using different methods to form hydrates, including the formation of hydrates in thin films obtained using the vapor deposition method.

### Acknowledgments

This research was financially supported by the Ministry of Science and Higher Education of the Republic of Kazakhstan as part of the grant AP15473758

## References

1. Smith, S.J., M.L. Wigley, Global Warming Potentials: 1. Climatic Implications of Emissions Reductions. *Climatic Change*, vol. 44, 445–457 (2000).
2. R.T. Pierrehumbert: “Short-Lived Climate Pollution.” *Annu. Rev. Earth Planet. Sci.* vol. 42, no. 1, pp. 341–379, 2014.
3. M.R. Edwards, J. McNeerney, and J.E. Trancik: “Testing emissions equivalency metrics against climate policy goals.” *Environ. Sci. Policy*. vol. 66, pp. 191–198, 2016.
4. D.P. Schrag: “Storage of Carbon Dioxide in Offshore Sediments.” *Science (80-. )*. vol. 325, no. 5948, pp. 1658–1659, 2009.
5. K.A. Kvenvolden: “Gas hydrates-geological perspective and global change.” *Rev. Geophys.* vol. 31, no. 2, pp. 173–187, 1993.
6. Y. Konno, T. Fujii, A. Sato, K. Akamine, M. Naiki, Y. Masuda, K. Yamamoto, and J. Nagao: “Key Findings of the World’s First Offshore Methane Hydrate Production Test off the Coast of Japan: Toward Future Commercial Production.” *Energy & Fuels*. vol. 31, no. 3, pp. 2607–2616, 2017.
7. J. Li, J. Ye, X. Qin, H. Qiu, N. Wu, H. Lu, W. Xie, J. Lu, F. Peng, Z. Xu, C. Lu, Z. Kuang, J. Wei, Q. Liang, H. Lu, and B. Kou: “The first offshore natural gas hydrate production test in South China Sea.” *China Geol.* vol. 1, no. 1, pp. 5–16, 2018.
8. E.D. Sloan Jr., C.A. Koh, and C.A. Koh: “Clathrate Hydrates of Natural Gases.” *CRC Press*, 2007.
9. M. Ricaurte, C. Dicharry, X. Renaud, and J.-P. Torr : “Combination of surfactants and organic compounds for boosting CO<sub>2</sub> separation from natural gas by clathrate hydrate formation.” *Fuel*. vol. 122, pp. 206–217, 2014.
10. S. Tomita, S. Akatsu, and R. Ohmura: “Experiments and thermodynamic simulations for continuous separation of CO<sub>2</sub> from CH<sub>4</sub> + CO<sub>2</sub> gas mixture utilizing hydrate formation.” *Appl. Energy*. vol. 146, pp. 104–110, 2015.
11. H. Mimachi, M. Takahashi, S. Takeya, Y. Gotoh, A. Yoneyama, K. Hyodo, T. Takeda, and T. Murayama: “Effect of Long-Term Storage and Thermal History on the Gas Content of Natural Gas Hydrate Pellets under Ambient Pressure.” *Energy & Fuels*. vol. 29, no. 8, pp. 4827–4834, 2015.
12. B.K. Malla, G. Vishwakarma, S. Chowdhury, P. Selvarajan, and T. Pradeep: “Formation of Ethane Clathrate Hydrate in Ultrahigh Vacuum by Thermal Annealing.” *J. Phys. Chem. C*. vol. 126, no. 42, pp. 17983–17989, 2022.
13. M. Li, K. Li, L. Yang, Y. Su, J. Zhao, and Y. Song: “Evidence of Guest–Guest Interaction in Clathrates Based on In Situ Raman Spectroscopy and Density Functional Theory.” *J. Phys. Chem. Lett.* vol. 13, no. 1, pp. 400–405, 2022.
14. H. Koide, M. Takahashi, H. Tsukamoto, and Y. Shindo: “Self-trapping mechanisms of carbon dioxide in the aquifer disposal.” *Energy Convers. Manag.* vol. 36, no. 6–9, pp. 505–508, 1995.
15. B. Tohidi, J. Yang, M. Salehabadi, R. Anderson, and A. Chapoy: “CO<sub>2</sub> Hydrates Could Provide Secondary Safety Factor in Subsurface Sequestration of CO<sub>2</sub>.” *Environ. Sci. Technol.* vol. 44, no. 4, pp. 1509–1514, 2010.
16. J. Zheng, Z.R. Chong, M.F. Qureshi, and P. Linga: “Carbon Dioxide Sequestration via Gas Hydrates: A Potential Pathway toward Decarbonization.” *Energy & Fuels*. vol. 34, no. 9, pp. 10529–10546, 2020.
17. M.F. Qureshi, V. Dhamu, A. Usadi, T.A. Barckholtz, A.B. Mhadeshwar, and P. Linga: “CO<sub>2</sub> Hydrate Formation Kinetics and Morphology Observations Using High-Pressure Liquid CO<sub>2</sub> Applicable to Sequestration.” *Energy & Fuels*. vol. 36, no. 18, pp. 10627–10641, 2022.
18. T. Takahashi and T. Sato: “Inclusive environmental impact assessment indices with consideration of public acceptance: Application to power generation technologies in Japan.” *Appl. Energy*. vol. 144, pp. 64–72, 2015.
19. P. Englezos, N. Kalogerakis, P.D. Dholabhai, and P.R. Bishnoi: “Kinetics of formation of methane and ethane gas hydrates.” *Chem. Eng. Sci.* vol. 42, no. 11, pp. 2647–2658, 1987.
20. C.P. Ribeiro and P.L.C. Lage: “Gas-Liquid Direct-Contact Evaporation: A Review.” *Chem. Eng. Technol.* vol. 28, no. 10, pp. 1081–1107, 2005.
21. P. Linga, R. Kumar, and P. Englezos: “Gas hydrate formation from hydrogen/carbon dioxide and nitrogen/carbon dioxide gas mixtures.” *Chem. Eng. Sci.* vol. 62, no. 16, pp. 4268–4276, 2007.
22. J. Cai, Y. Zhang, C.-G. Xu, Z.-M. Xia, Z.-Y. Chen, and X.-S. Li: “Raman spectroscopic studies on carbon dioxide separation from fuel gas via clathrate hydrate in the presence of tetrahydrofuran.” *Appl. Energy*. vol. 214, pp. 92–102, 2018.
23. X.-S. Li, C.-G. Xu, Z.-Y. Chen, and H.-J. Wu: “Hydrate-based pre-combustion carbon dioxide capture process in the system with tetra-n-butyl ammonium bromide solution in the presence of cyclopentane.” *Energy*. vol. 36, no. 3, pp. 1394–1403, 2011.
24. H. Liu, J. Wang, G. Chen, B. Liu, A. Dandekar, B. Wang, X. Zhang, C. Sun, and Q. Ma: “High-efficiency separation of a CO<sub>2</sub>/H<sub>2</sub> mixture via hydrate formation in W/O emulsions in the presence of cyclopentane and TBAB.” *Int. J. Hydrogen Energy*. vol. 39, no. 15, pp. 7910–7918, 2014.

25. R. Kumar, H. Wu, and P. Englezos: "Incipient hydrate phase equilibrium for gas mixtures containing hydrogen, carbon dioxide and propane." *Fluid Phase Equilib.* vol. 244, no. 2, pp. 167–171, 2006.
26. X. Wang, F. Zhang, and W. Lipiński: "Research progress and challenges in hydrate-based carbon dioxide capture applications." *Appl. Energy.* vol. 269, pp. 114928, 2020.
27. T. Uchida: "Physical property measurements on CO<sub>2</sub> clathrate hydrates. Review of crystallography, hydration number, and mechanical properties." *Waste Manag.* vol. 17, no. 5–6, pp. 343–352, 1998.
28. Y.-J. Lee, K.W. Han, J.S. Jang, T.-I. Jeon, J. Park, T. Kawamura, Y. Yamamoto, T. Sugahara, T. Vogt, J.-W. Lee, Y. Lee, and J.-H. Yoon: "Selective CO<sub>2</sub> Trapping in Guest-Free Hydroquinone Clathrate Prepared by Gas-Phase Synthesis." *ChemPhysChem.* vol. 12, no. 6, pp. 1056–1059, 2011.
29. D.J. Arismendi-Arrieta, Á. Valdés, and R. Prosmiiti: "A Systematic Protocol for Benchmarking Guest-Host Interactions by First-Principles Computations: Capturing CO<sub>2</sub> in Clathrate Hydrates." *Chem. – A Eur. J.* vol. 24, no. 37, pp. 9353–9363, 2018.
30. A. Aldiyarov, M. Aryutkina, A. Drobyshev, and V. Kurnosov: "IR spectroscopy of ethanol in nitrogen cryomatrices with different concentration ratios." *Low Temp. Phys.* vol. 37, no. 6, pp. 524–531, 2011.
31. A. Sanz-Hervás, E. Iborra, M. Clement, J. Sangrador, and M. Aguilar: "Influence of crystal properties on the absorption IR spectra of polycrystalline AlN thin films." *Diam. Relat. Mater.* vol. 12, no. 3–7, pp. 1186–1189, 2003.
32. I. Karamancheva, V. Stefov, B. Šoptrajanov, G. Danev, E. Spasova, and J. Assa: "FTIR spectroscopy and FTIR microscopy of vacuum-evaporated polyimide thin films." *Vib. Spectrosc.* vol. 19, no. 2, pp. 369–374, 1999.
33. A. Oancea, O. Grasset, E. Le Menn, O. Bollengier, L. Bezacier, S. Le Mouélic, and G. Tobie: "Laboratory infrared reflection spectrum of carbon dioxide clathrate hydrates for astrophysical remote sensing applications." *Icarus.* vol. 221, no. 2, pp. 900–910, 2012.
34. E.M. Myshakin, W.A. Saidi, V.N. Romanov, R.T. Cygan, and K.D. Jordan: "Molecular Dynamics Simulations of Carbon Dioxide Intercalation in Hydrated Na-Montmorillonite." *J. Phys. Chem. C.* vol. 117, no. 21, pp. 11028–11039, 2013.
35. Á. Valdés, D.J. Arismendi-Arrieta, and R. Prosmiiti: "Quantum Dynamics of Carbon Dioxide Encapsulated in the Cages of the sI Clathrate Hydrate: Structural Guest Distributions and Cage Occupation." *J. Phys. Chem. C.* vol. 119, no. 8, pp. 3945–3956, 2015.
36. M. Tyliniski, Y.Z. Chua, M.S. Beasley, C. Schick, and M.D. Ediger: "Vapor-deposited alcohol glasses reveal a wide range of kinetic stability." *J. Chem. Phys.* vol. 145, no. 17, pp. 174506, 2016.
37. A. Shinbayeva, A. Drobyshev, and N. Drobyshev: "The standardization and certification procedures of cryogenic equipment in Kazakhstan." *Low Temp. Phys.* vol. 41, no. 7, pp. 571–573, 2015.
38. A. Aldiyarov, A. Nurmukan, D. Sokolov, and E. Korshikov: "Investigation of vapor cryodeposited glasses and glass transition of tetrachloromethane films." *Appl. Surf. Sci.* vol. 507, pp. 144857, 2020.
39. A. Drobyshev, A. Aldiyarov, A. Nurmukan, D. Sokolov, and A. Shinbayeva: "Structure transformations in thin films of CF<sub>3</sub>-CF<sub>2</sub> cryodeposited. Is there a glass transition and what is the value of T<sub>g</sub>?" *Appl. Surf. Sci.* vol. 446, pp. 196–200, 2018.
40. A. Drobyshev, A. Aldiyarov, D. Sokolov, and A. Shinbayeva: "Refractive indices and density of cryovacuum-deposited thin films of methane in the vicinity of the  $\alpha$ - $\beta$ -transition temperature." *Low Temp. Phys.* vol. 43, no. 6, pp. 724–727, 2017.
41. A.U. Aldiyarov, D.Y. Sokolov, A.Y. Nurmukan, and M.A. Ramos: "Refractive Index at Low Temperature of Tetrachloromethane and Tetrafluoroethane Cryovacuum Condensates." *ACS Omega.* vol. 5, no. 20, pp. 11671–11676, 2020.
42. D.Y. Sokolov, D. Yerezhep, O. Vorobyova, M.A. Ramos, and A. Shinbayeva: "Optical Studies of Thin Films of Cryocondensed Mixtures of Water and Admixture of Nitrogen and Argon." *Materials (Basel).* vol. 15, no. 21, pp. 7441, 2022.
43. D.Y. Sokolov, D. Yerezhep, O. Vorobyova, O. Golikov, and A.U. Aldiyarov: "Infrared Analysis and Effect of Nitrogen and Nitrous Oxide on the Glass Transition of Methanol Cryofilms." *ACS Omega.* 2022.
44. E. Dartois and B. Schmitt: "Carbon dioxide clathrate hydrate FTIR spectrum." *Astron. Astrophys.* vol. 504, no. 3, pp. 869–873, 2009.
45. L.S. Rothman and L.D.G. Young: "Infrared energy levels and intensities of carbon dioxide—II." *J. Quant. Spectrosc. Radiat. Transf.* vol. 25, no. 6, pp. 505–524, 1981.
46. M. BERNSTEIN, D. CRUIKSHANK, and S. SANDFORD: "Near-infrared laboratory spectra of solid HO/CO and CHO/CO ice mixtures." *Icarus.* vol. 179, no. 2, pp. 527–534, 2005.
47. S.A. Sandford and L.J. Allamandola: "The physical and infrared spectral properties of CO<sub>2</sub> in astrophysical ice analogs." *Astrophys. J.* vol. 355, pp. 357, 1990.
48. C.E. Bryson, V. Cazarra, and L.L. Levenson: "Sublimation rates and vapor pressures of water, carbon dioxide, nitrous oxide, and xenon." *J. Chem. Eng. Data.* vol. 19, no. 2, pp. 107–110, 1974.